15th EVN Symposium & Users Meeting, 11-15 July 2022, Cork, Ireland

Multi-Frequency Imaging Results of 453 Extragalactic ICRF-3 Radio Sources from Multi Epoch, Near-Simultaneous Astrometric VLBA Observations

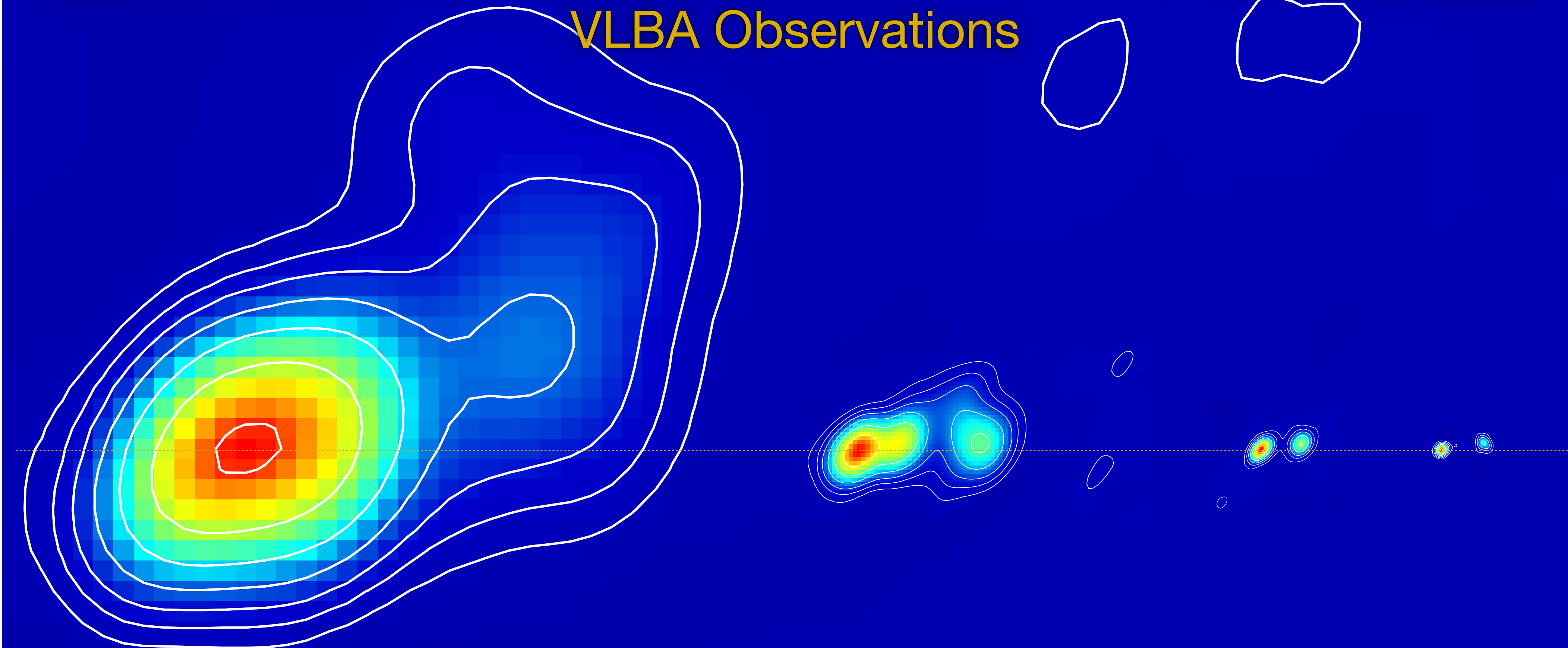

2351+456 - images from May 2021 at S, X, K and Q-band

Aletha de Witt, South African Radio Astronomy Observatory (SARAO), South Africa

C. S. Jacobs (1), D. Gordon (2), L. Hunt (2), M. Johnson (2)

(1) Jet Propulsion Laboratory, California Institute of Technology/NASA, United States, (2) United States Naval Observatory (USNO), United States

Context: Celestial Reference Frames

Current standard International Celestial Reference Frame (ICRF):

- ICRF-3 adopted by IAU Aug 2018 (Charlot et al, 2020)
- High precision VLBI astrometric measurements of positions of > 5000 AGN
- First multi-frequency frame with catalogs at S/X, K, and X/Ka-band

- S/X-band	**(8 GHz, 3.6 cm)**	
- K-band	**(24 GHz, 1.2 cm)**	~100 µas or better precision
- X/Ka-band	**(32 GHz, 0.9 cm)**	

★ **We are investigating the potential for a Q-band CRF (43 GHz, 0.7 cm)**

Motivation for higher frequency bands:

- S/X-band being hurt by S-band RFI issues
- Solar plasma effect reduced as 1/ freq squared and allows observations closer to Sun
- Allows observations closer to Galactic plane
- Provides calibrators for VLBI phase-referencing at higher radio frequencies
- *K-band provides EVN with precise staton locations* (Gomez et al, 2020)
- Improvement in interferometer resolution relative to standard S/X-band

★ More compact source morphology and reduced core-shift effect

We conducted S/X, K and Q-band astrometric/imaging observations:

- Three epochs of near-simultaneous VLBA observations between Apr and Jun 2021

★ Imaging allows us to directly compare the source structure at S, X, K, and Q-band

Astrophysics: Source Structure

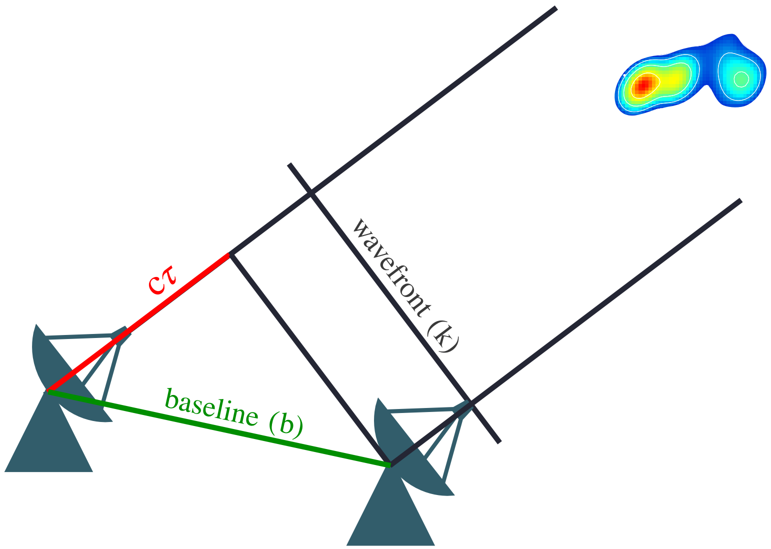

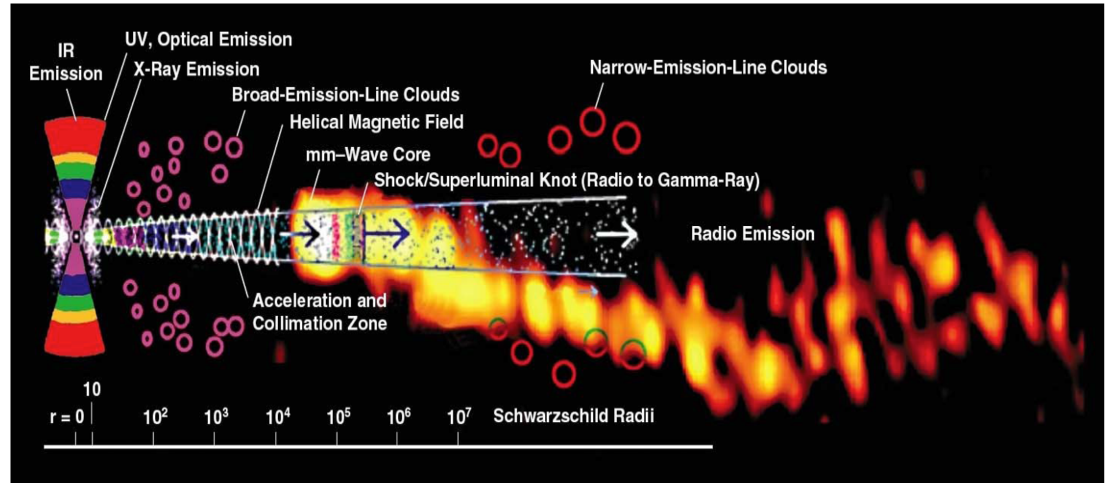

Credits: Alan Marscher, `Relativistic Jets in Active Galactic Nuclei and their relationship to the Central Engine,' Proc. of Science,VI Microquasar Workshop: Microquasars & Beyond, Societa del Casino, Como, Italy, 18-22 Sep 2006. Overlay (not to scale): 3 mm radio image of the blazar 3C454.3 (Krichbaum et al. 1999).

Primary observable for geodetic and astrometric VLBI is the delay (τ).

- By measuring and modeling τ for each baseline of the network, we can precisely infer the position of the observed radio sources
- τ is dominated by a geometric component, with other contributions from the atmosphere, instrumetal effects, relativistic effects and ★**source structure (not modelled)**
- Source structure and its variability can introduce significant errors in the astrometric VLBI delay measurements and instabilities in the individual source positions (Charlot et al. 1990)

Apparent source structure in AGN is a function of frequency - main reason is frequency dependent opacity

- Core components generally have flatter radio spectra than the jets, so at higher frequencies the core components tend to be dominant - source morphology generally more compact
- Can also contribute to the frequency dependent shift of the VLBI core position - with observed position of the peak brightness point moving closer to the central black hole as the frequency increases (e.g., Sokolovsky et al. 2011)
- However, going to lower frequencies reduces the ability to detect structure and desensitizes the baseline to structure

Observations: VLBA S/X, K, and Q-band

Near-simultaneous VLBA 24-hr observations at S/X, K, and Q band of 453 AGN

- **Calibration, imaging:** using AIPS (Greisen 2003) and DIFMAP (Deller et al. 2011)
- **Modelfitting to calibrated visibilities:** core & 2nd brightest component using DIFMAP
- **Modelfitting to CLEAN component locations:** using PYTHON

Motivation: to assess the astrometric source suitability at each frequency band

1. We will show how source structure compares amongst all four bands
2. We will assess the potential advantages of higher radio frequencies for CRF work
3. We compare the jet direction to the astrometric offset direction from X and K band

Band	Date (2021)	Ref freq	Data Rate	Bandwidth	Polarization	θ_{VLBA}
S-band	16 Apr, 24 May, 13 Jun	2.316 GHz	2 Gbps	4 x 64 MHz	LCP	3.12 mas
X-band	16 Apr, 24 May, 13 Jun	8.668 GHz	2 Gbps	12 x 64 MHz	LCP	0.82 mas
K-band	18 Apr, 23 May, 12 Jun	23.568 GHz	4 Gbps	4 x 128 MHz	LCP/RCP	0.30 mas
Q-band	19 Apr, 25 May, 14 Jun	43.169 GHz	4 Gbps	4 x 128 MHz	LCP/RCP	0.17 mas

Imaging and Modelfitting: NRAO140

NRF National Research Foundation
SARAO South African Radio Astronomy Observatory

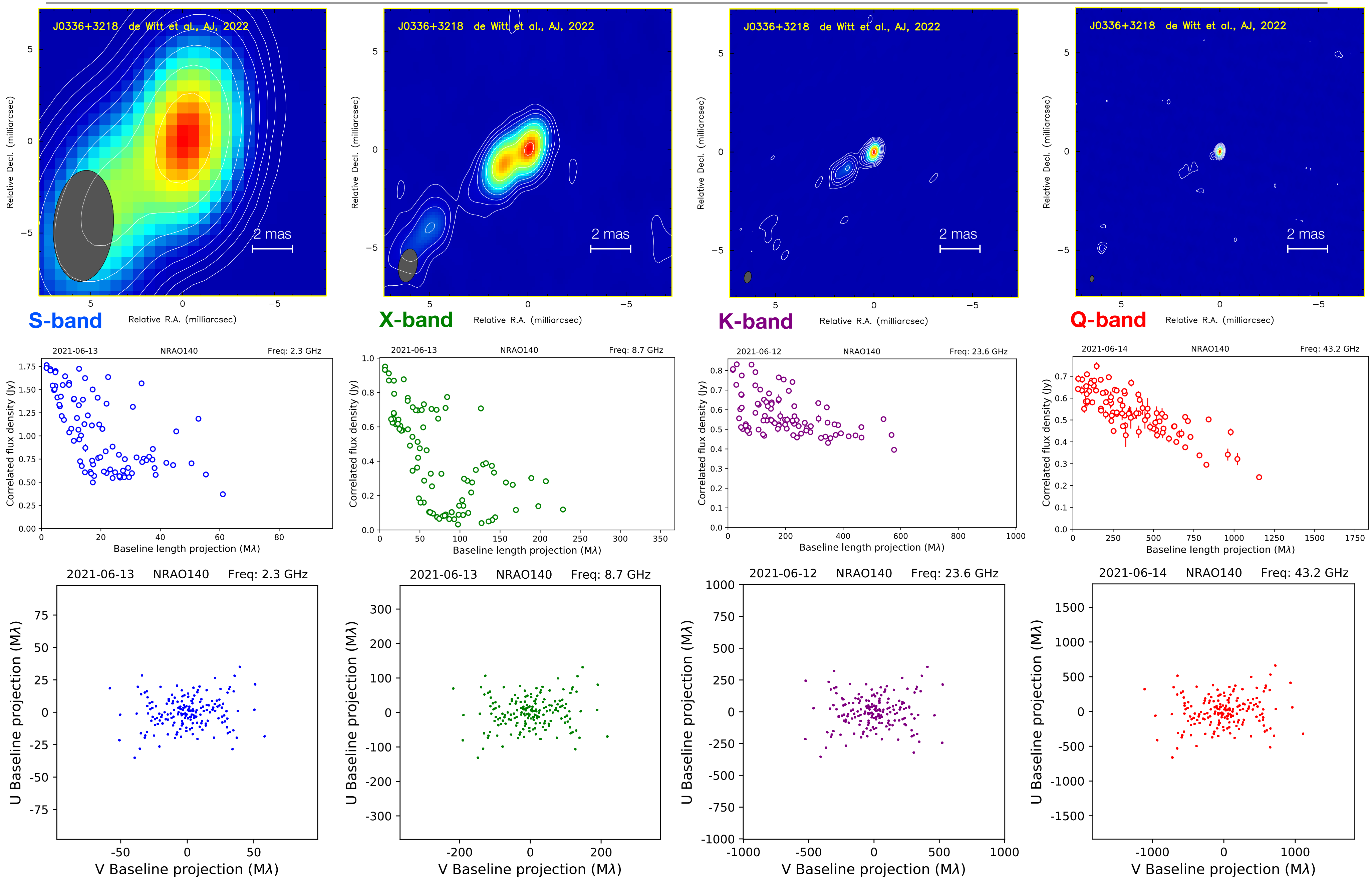

Imaging and Modelfitting: NRAO140

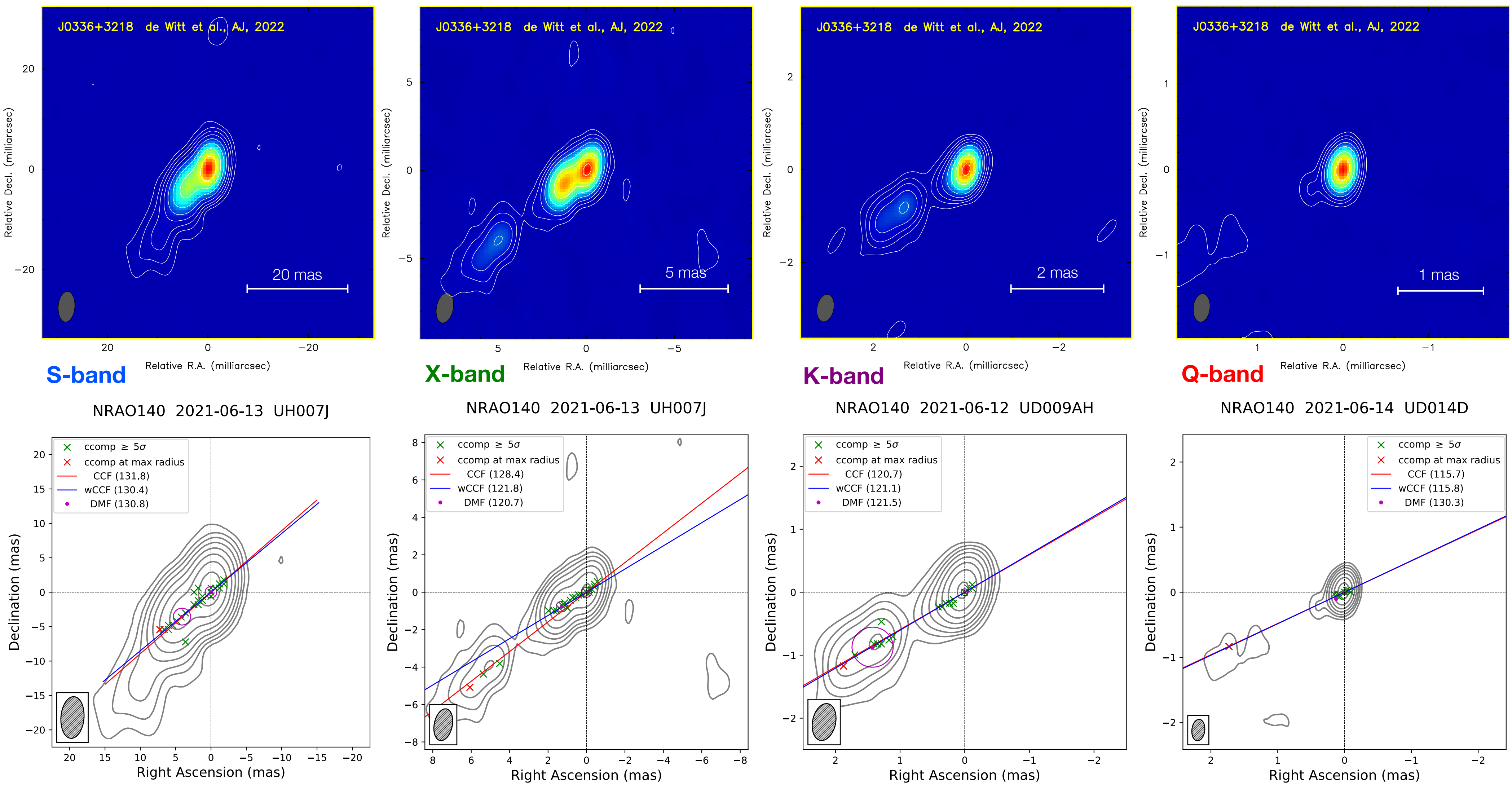

Structure Metrics: Compactness

Peak Brightness

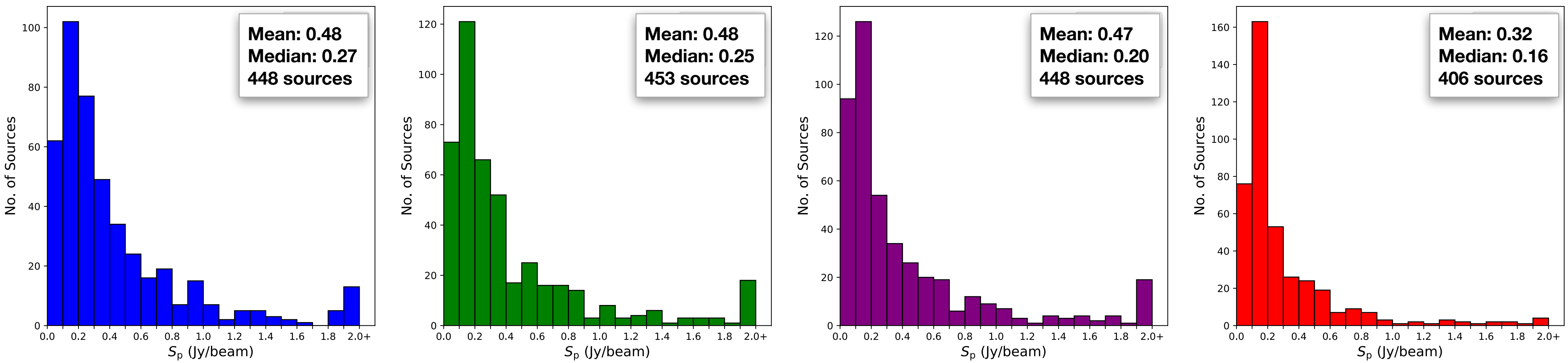

Compactness Ratio (C_1) —> peak brightness/CLEAN flux density

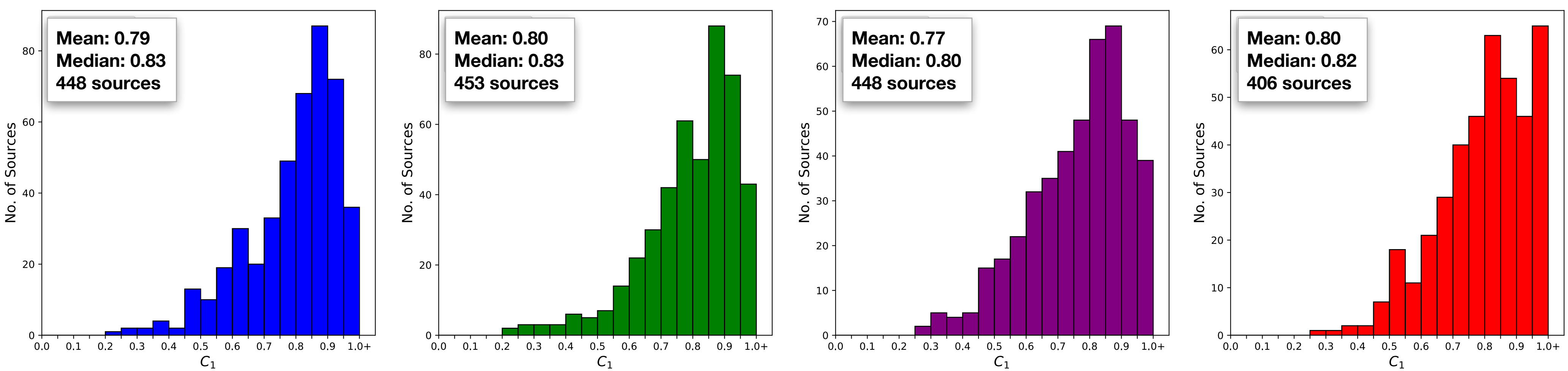

Structure Metrics: Correlated Flux Ratio

Correlated Flux Density Ratio (C_3) —> average long baselines/short baselines?

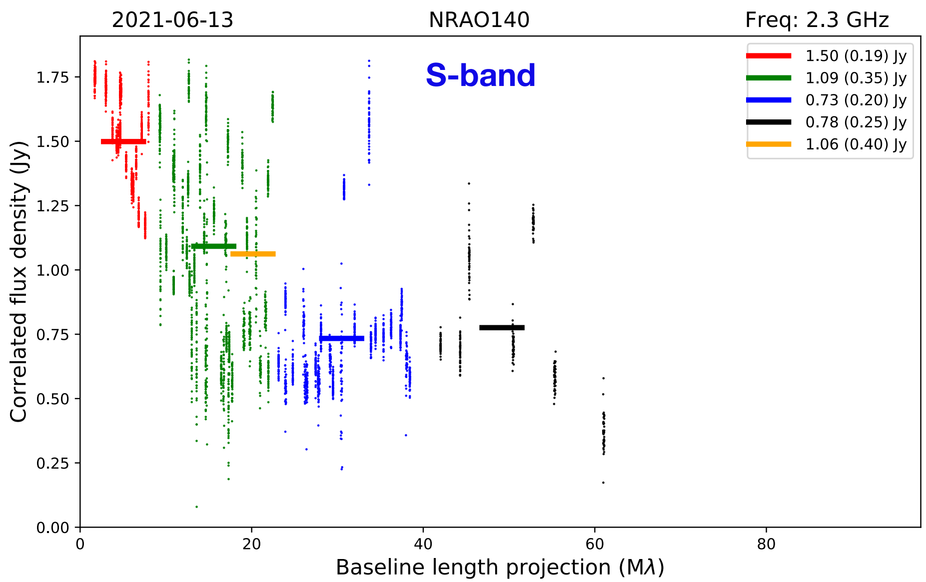

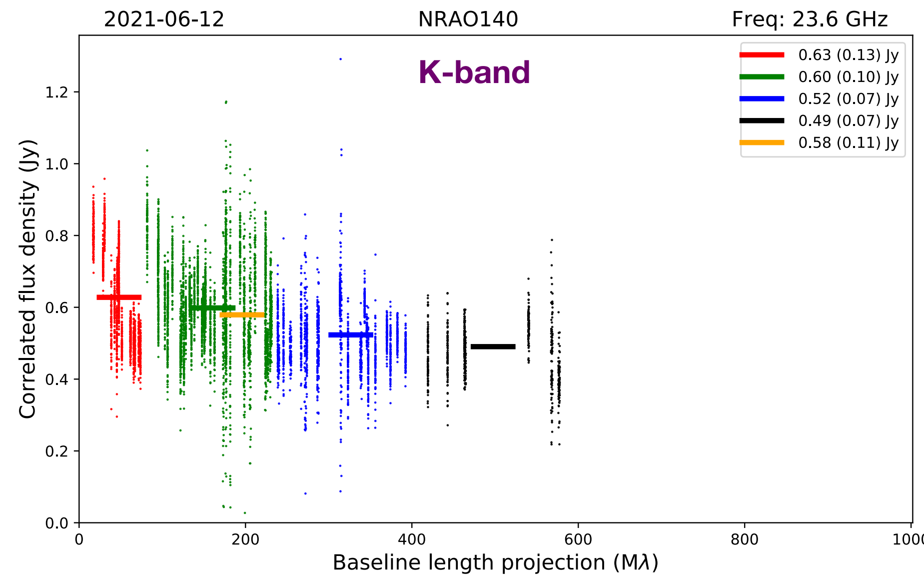

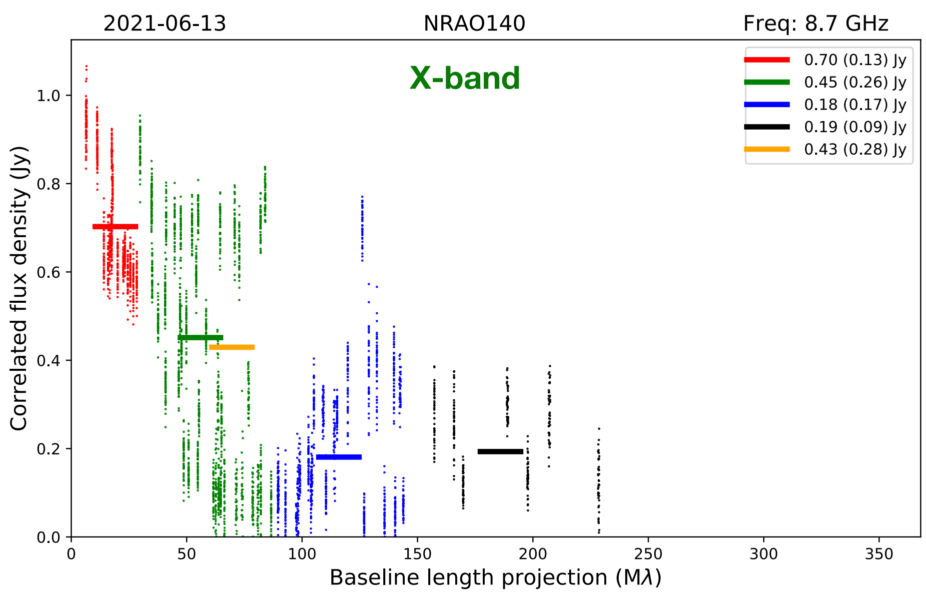

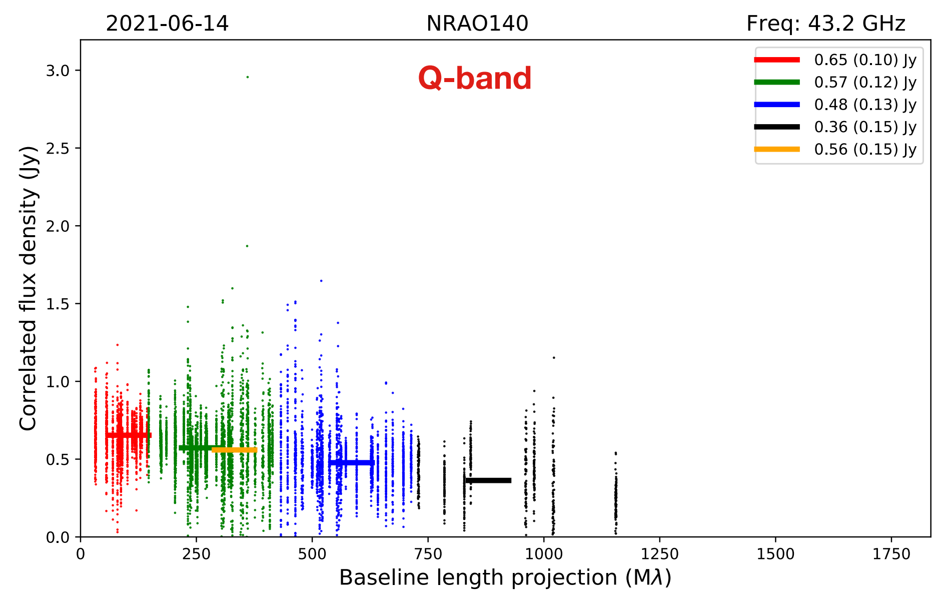

Structure Metrics: Structure Index

Structure Index (SI) —> derived from median value of structural delay values for all possible Earth-based baselines (Fey & Charlot 1997, 2000, McCallum et al., 2020) $\mathrm{SI} = 1 + 2 \times log_{10}(\tau_{\mathrm{median}})$

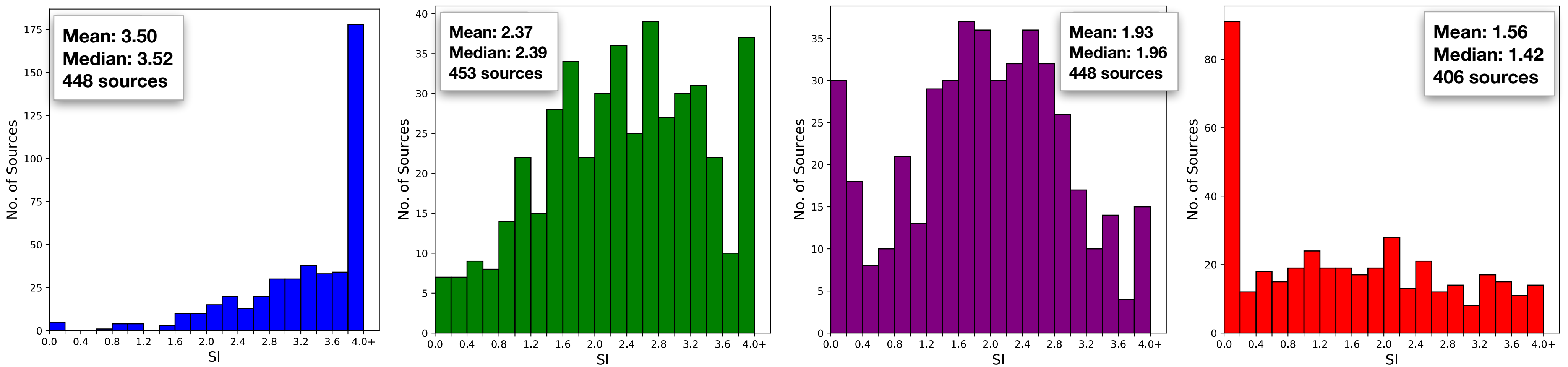

Structure Metrics: Structure Index

Structure Index (SI) —> derived from median value of structural delay values for all possible Earth-based baselines (Fey & Charlot 1997, 2000, McCallum et al., 2020) $\mathrm{SI} = 1 + 2 \times log_{10}(\tau_{\text{median}})$

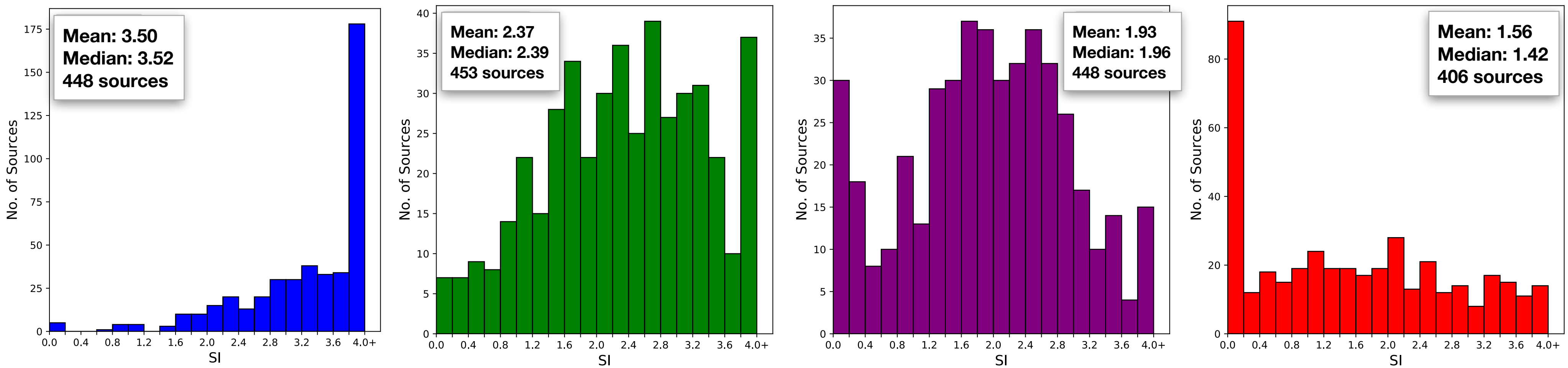

Structural delay or structure correction maps —> derived from source model underlying the VLBI image (CLEAN comp's) for all possible Earth-based baselines

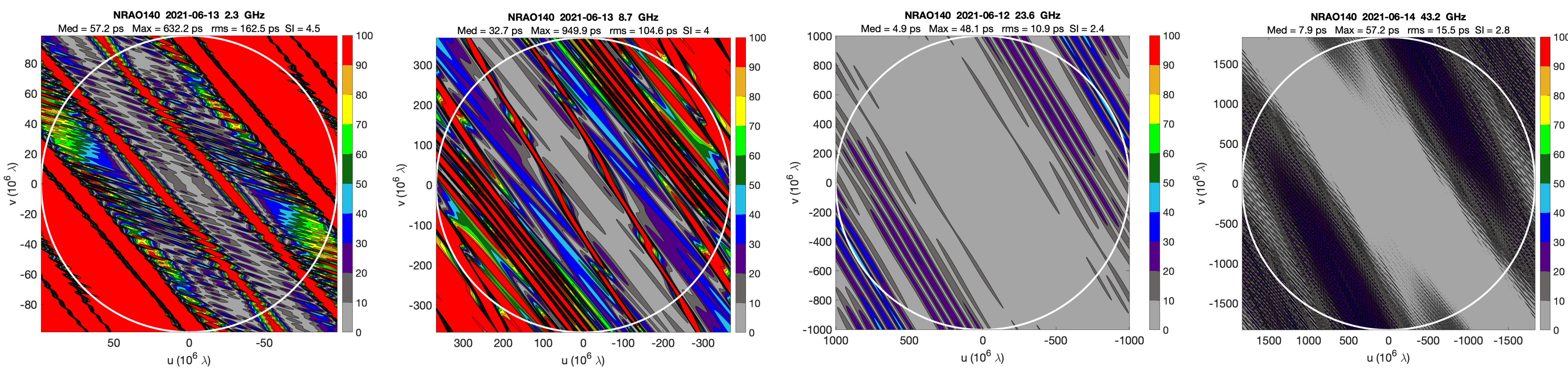

Structure Metrics: Structure Index

Structure Index (SI) —> derived from median value of structural delay values for all possible Earth-based baselines (Fey & Charlot 1997, 2000, McCallum et al., 2020) $\mathrm{SI} = 1 + 2 \times log_{10}(\tau_{\mathrm{median}})$

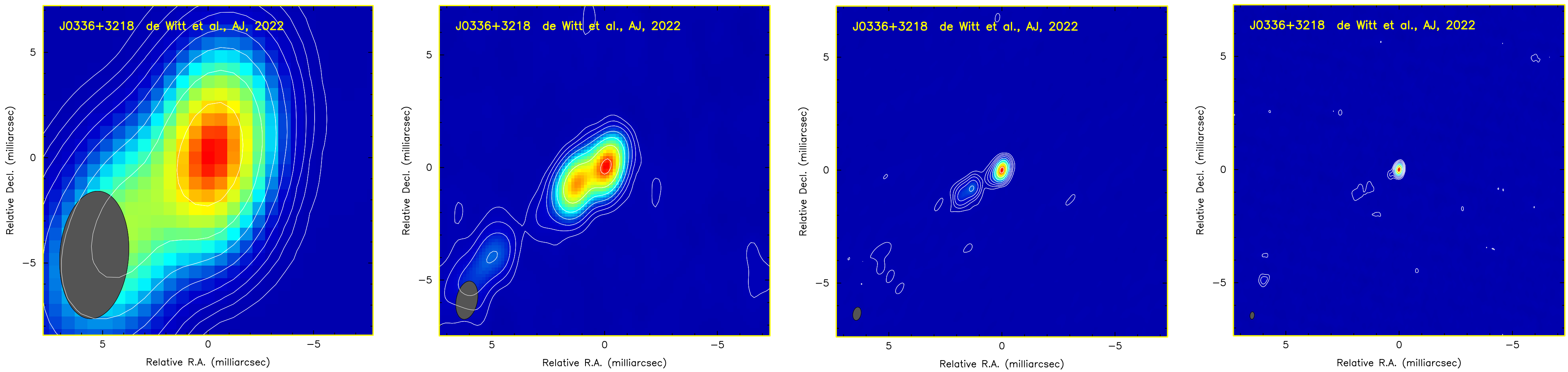

Structural delay or structure correction maps —> derived from source model underlying the VLBI image (CLEAN comp's) for all possible Earth-based baselines

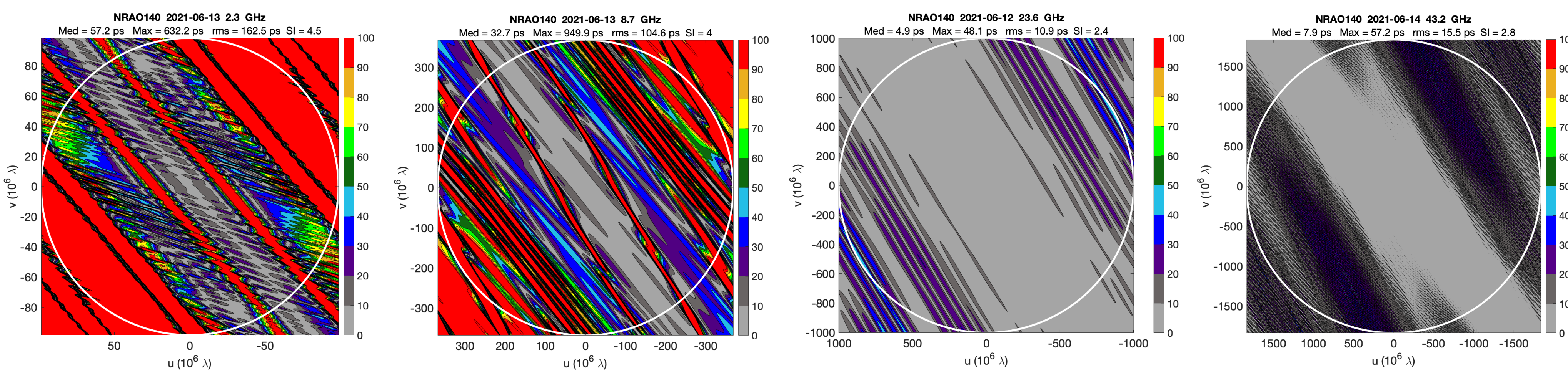

Astrometric Offsets:

X and K-band

We compare the direction of the extended emission from modelftting to the astrometric offset direction obtained from the X and K-band α cos(δ) and δ coordinates **(de Witt et al. 2022)**

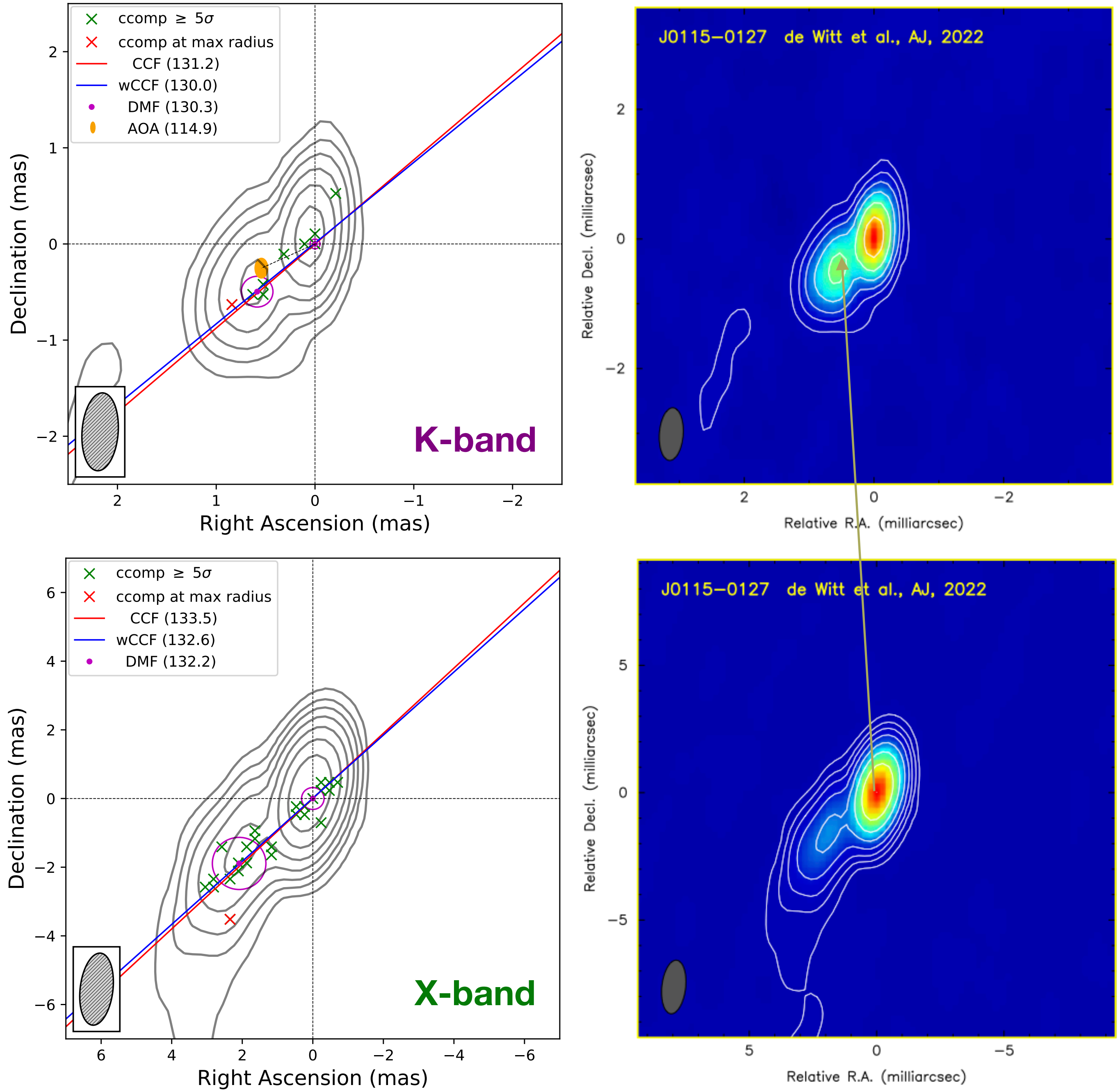

0112-017

AOA = astrometric offset angle
DMF = DIFMAP modelfit angle
CCF = angle from fit to CLEAN component locations
wCCF = angle from flux-weighted fit to CLEAN component locations.

Astrometric Offsets:

X and K-band

We compare the direction of the extended emission from modelftting to the astrometric offset direction obtained from the X and K-band α cos(δ) and δ coordinates **(de Witt et al. 2022)**

Algorithms give anti-parallel jet directions for X-band. Are we misidentifying the X-band core?

1214+588

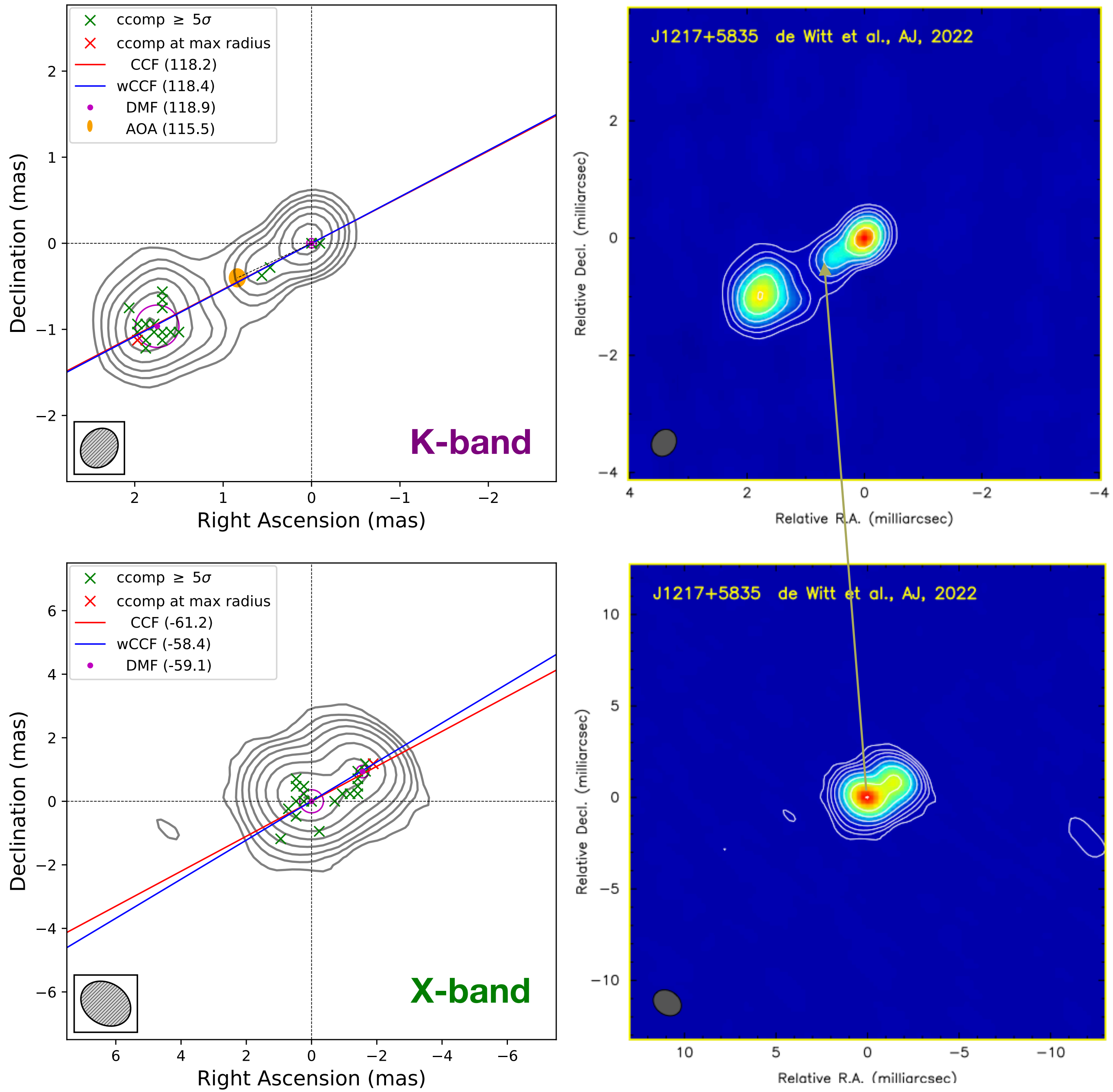

AOA = astrometric offset angle
DMF = DIFMAP modelfit angle
CCF = angle from fit to CLEAN component locations
wCCF = angle from flux-weighted fit to CLEAN component locations.

Multi-Frequency Comparisons: Summary

- **We imaged 453 ICRF sources from near-simultaneous VLBA observations at S, X, K, and Q band - some observed at multiple epochs**
- **From the images we derived source properties such as flux density, compactness, structure index and jet directions**
- **We find that K-band flux densities are comparable to X-band, while Q-band flux densities are a factor of 1.5 times lower than X-band - why fewer sources were detected at Q-band**
- **All three bands show that ~80% of the flux is in the central core**
- **The Structure Index shows that on average sources have less structure and become more compact at K and Q-band**
- **Comparisons of sources with X and K-band astrometric offsets show that jet angles from imaging in many cases agree with directions of astrometric offset**
- **Where angles are anti-parallel, correctly identifying the core is key (e.g. sources where the core in the X-band image is NOT the strongest component)**
- **Multiple statistical measures show that K and Q band are better because of less structure, and that Q-band is viable for CRF work.**

Acknowledgements:
The VLBA is managed by NRAO, funded by the National Science Foundation, and operated under cooperative agreement by Associated Universities. The authors gratefully acknowledge use of the VLBA under the USNO's time allocation. This work supports USNO's ongoing research into the celestial reference frame and geodesy.
This work was supported by the South African Radio Astronomy Observatory (SARAO,) a facility of the National Research Foundation (NRF) of South Africa.

Thank You

Contact Details

Aletha de Witt
www.hartrao.ac.za
alet@hartrao.ac.za

Image credit: Ani Vermeulen, NASSP student 2014

Structure Metrics: Compactness

Peak Brightness

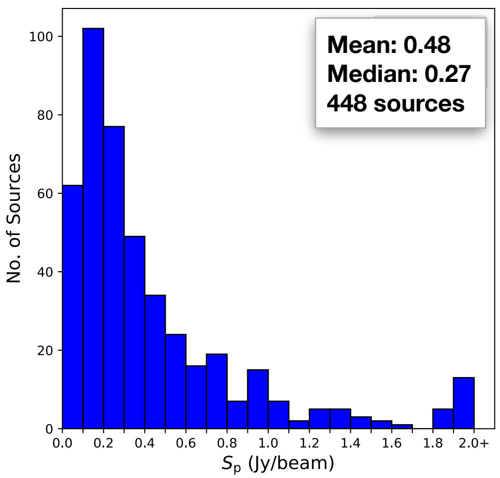

NRAO140: 0.96 Jy

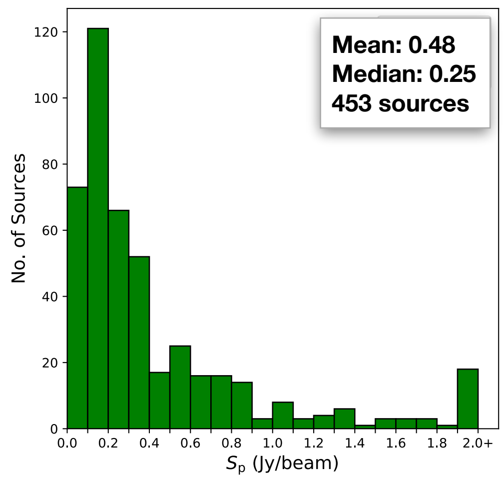

NRAO140: 0.38 Jy

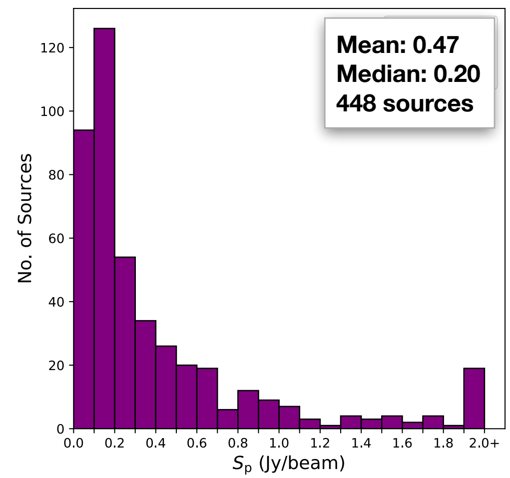

NRAO140: 0.57 Jy

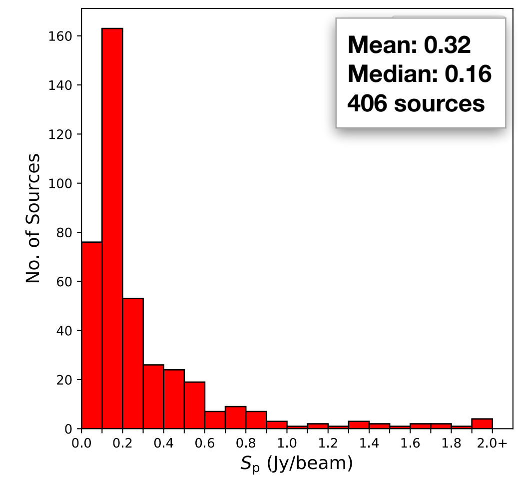

NRAO140: 0.56 Jy

Compactness Ratio (C_1) —> peak brightness/CLEAN flux density

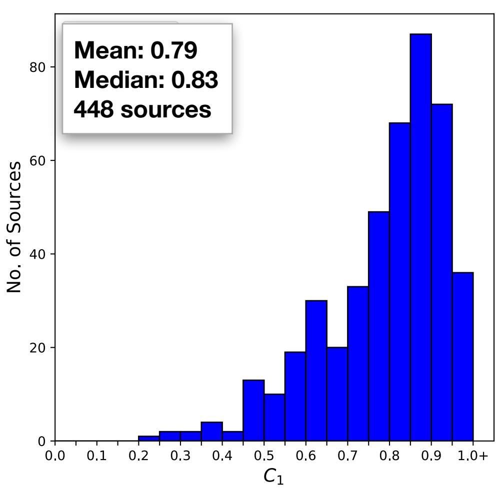

NRAO140: 0.55

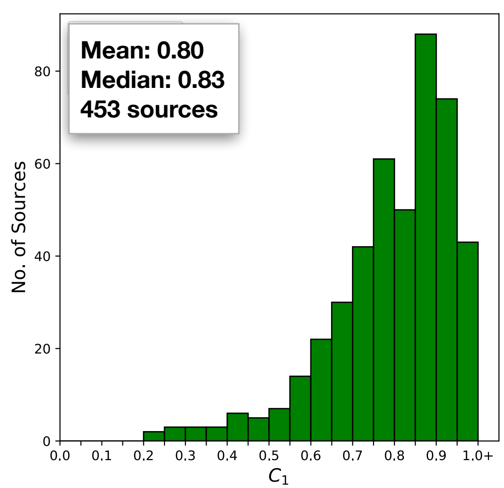

NRAO140: 0.41

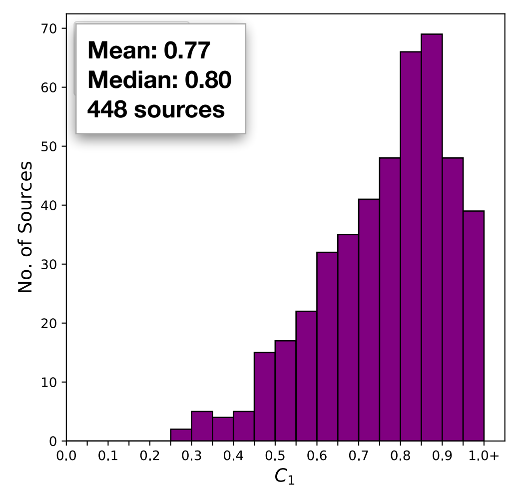

NRAO140: 0.71

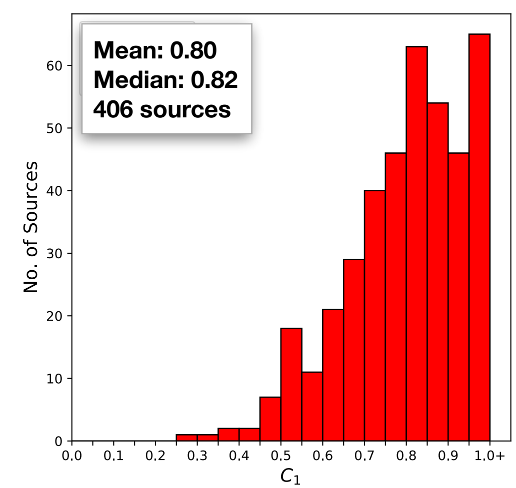

NRAO140: 0.78

Structure Metrics: Compactness

Peak Brightness

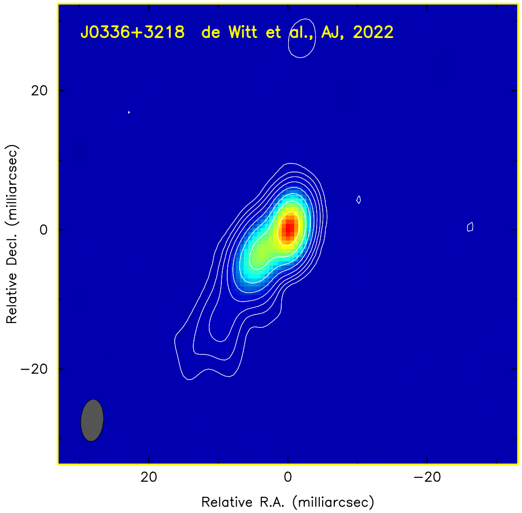

NRAO140: 0.96 Jy

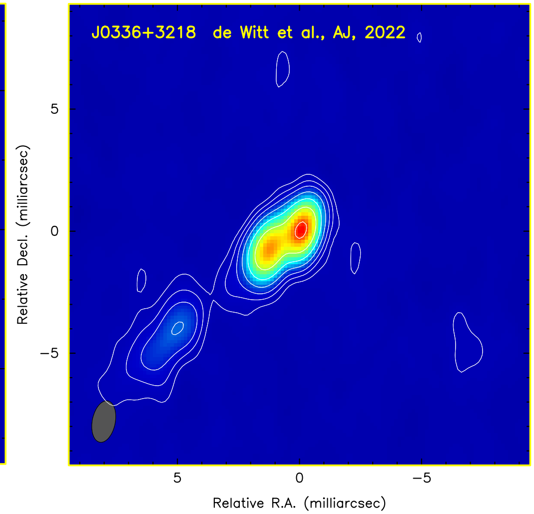

NRAO140: 0.38 Jy

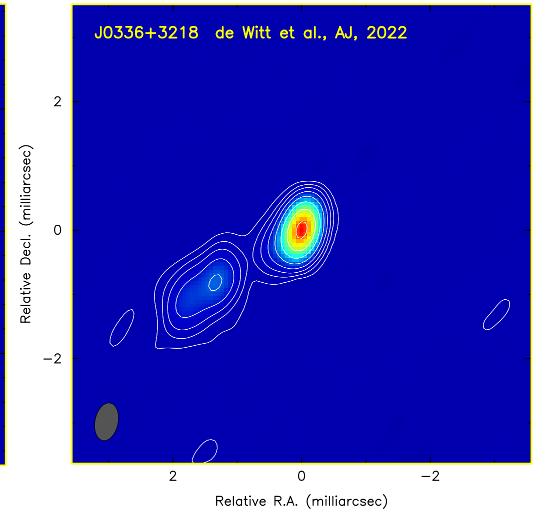

NRAO140: 0.57 Jy

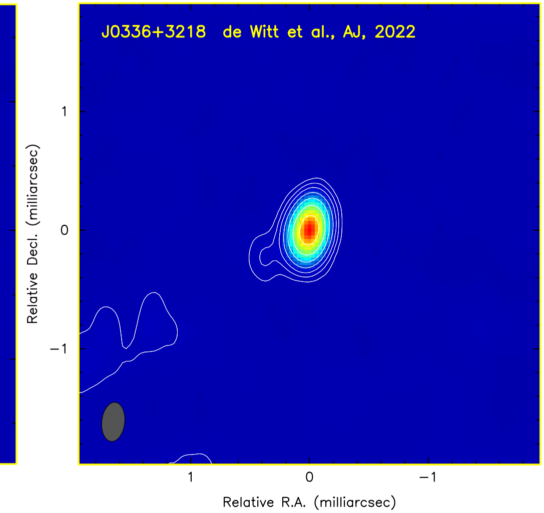

NRAO140: 0.56 Jy

Compactness Ratio (C_1) —> peak brightness/CLEAN flux density

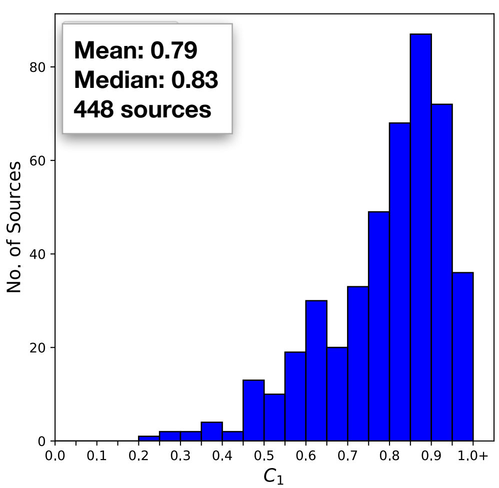

NRAO140: 0.55

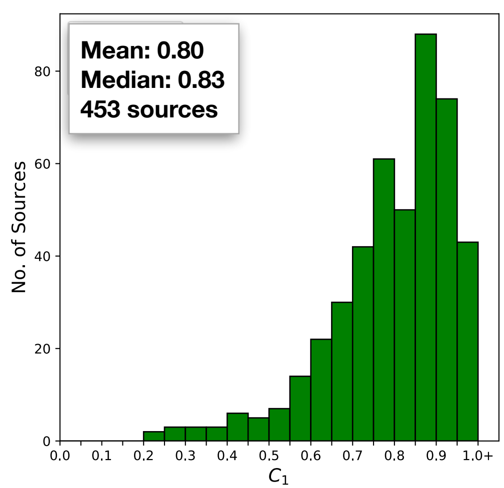

NRAO140: 0.41

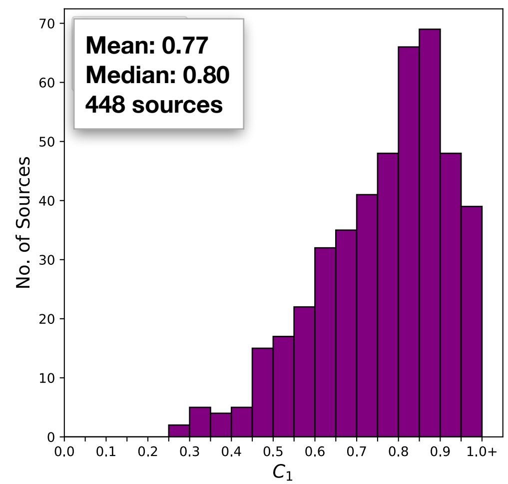

NRAO140: 0.71

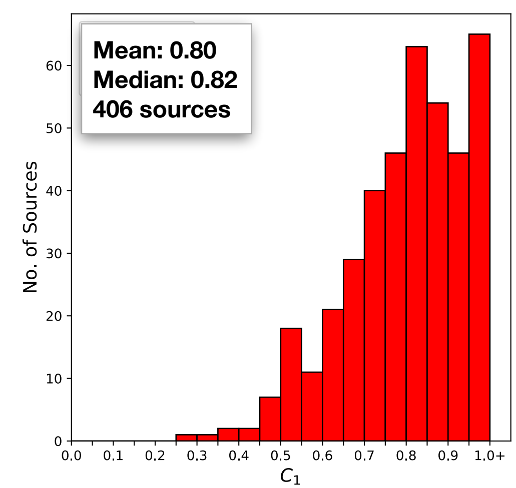

NRAO140: 0.78

Structure Metrics: Radial Extent

Flux Density Weighted Radial Extent (E, mas) —> extent of structure weighted by flux

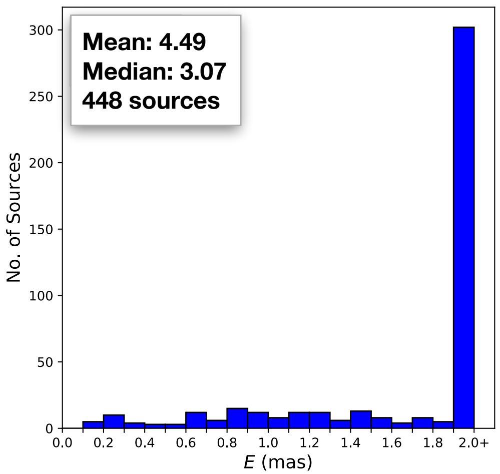

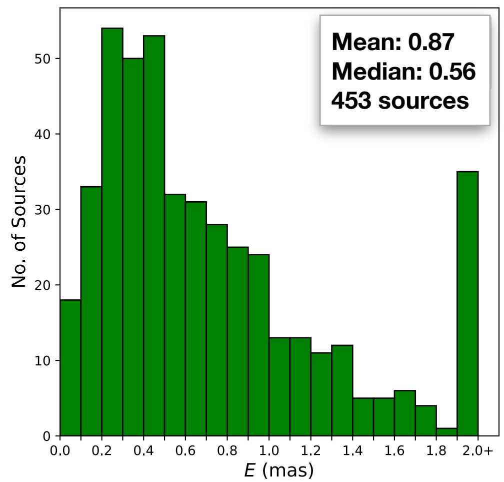

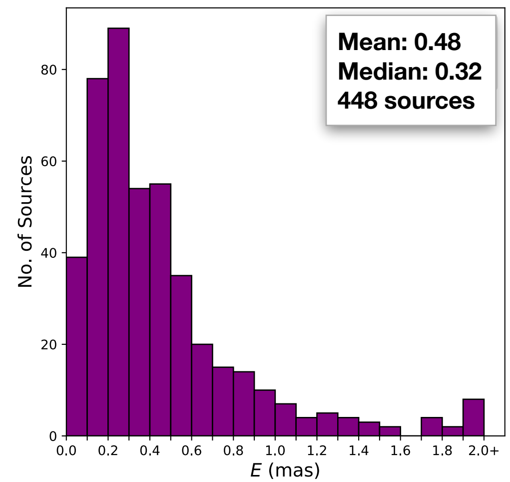

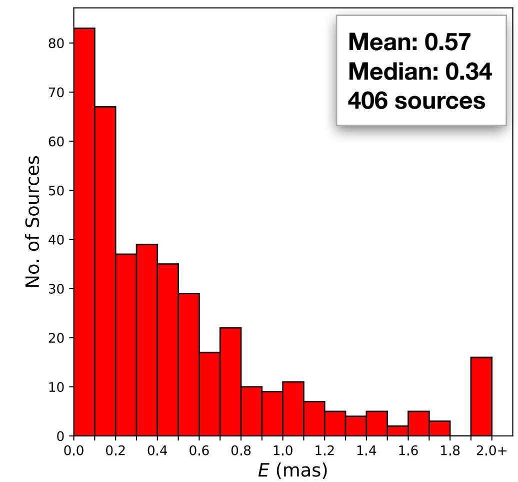

Flux Density Weighted Radial Extent $\leq 10 \times \theta_{\mathrm{FWHM}}$ (E_{10} , mas) —> spurious points filtered

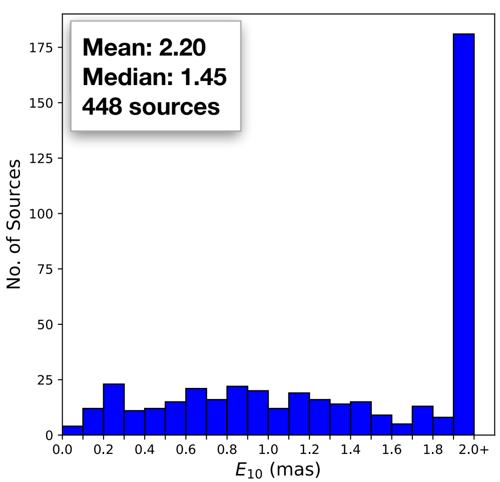

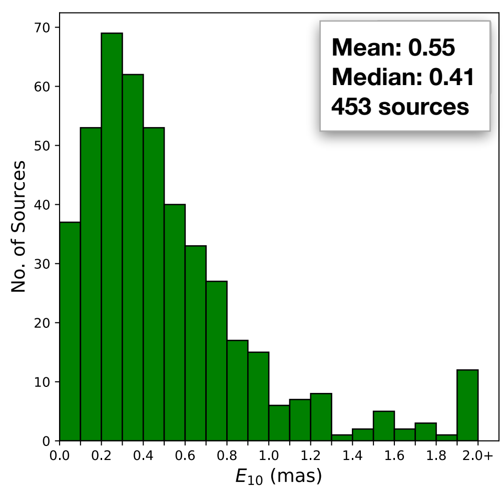

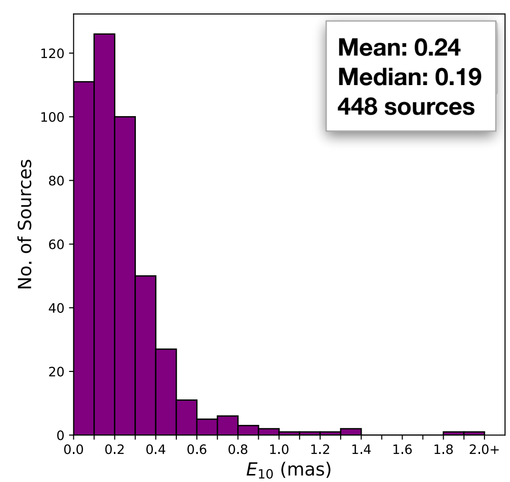

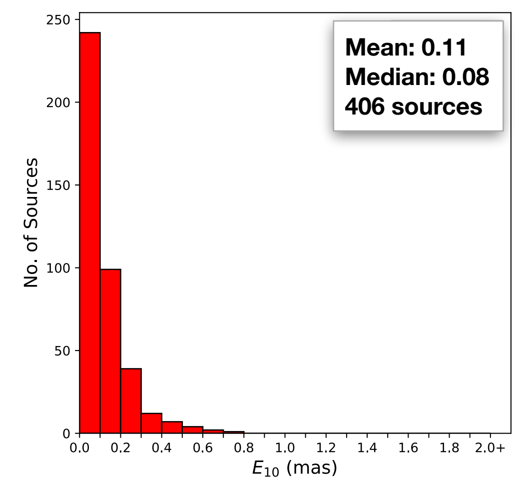

Structure Metrics: Radial Extent

NRF National Research Foundation | SARAO South African Radio Astronomy Observatory

Flux Density Weighted Radial Extent (E, mas) —> extent of structure weighted by flux

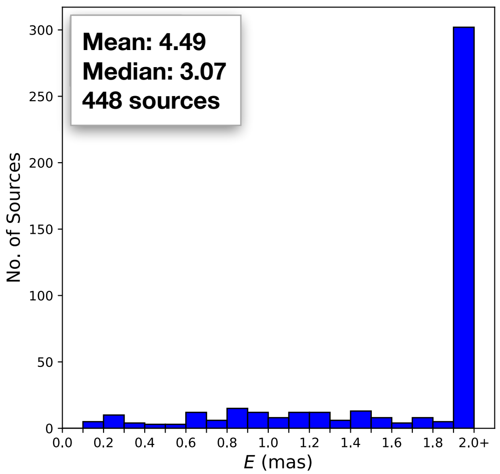

NRAO140: 4.29 mas

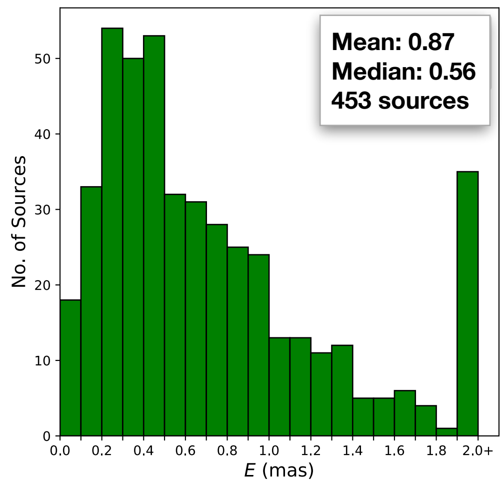

NRAO140: 1.54 mas

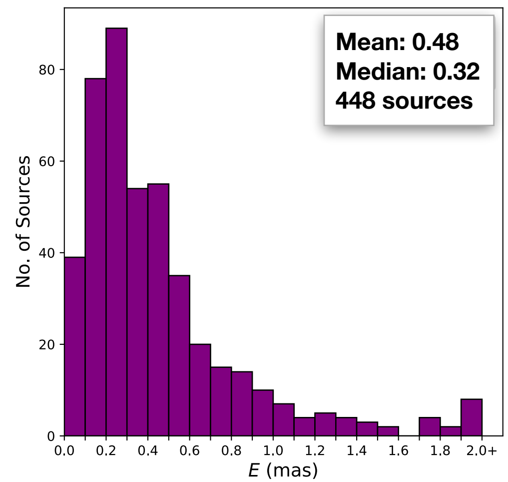

NRAO140: 0.52 mas

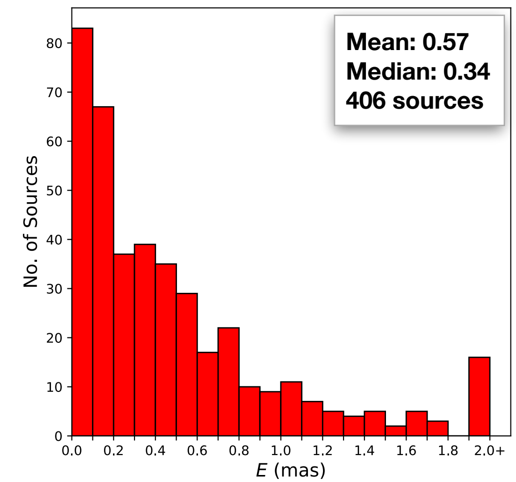

NRAO140: 0.54 mas

Flux Density Weighted Radial Extent $\leq 10 \times \theta_{FWHM}$ (E_{10} , mas) —> spurious points filtered

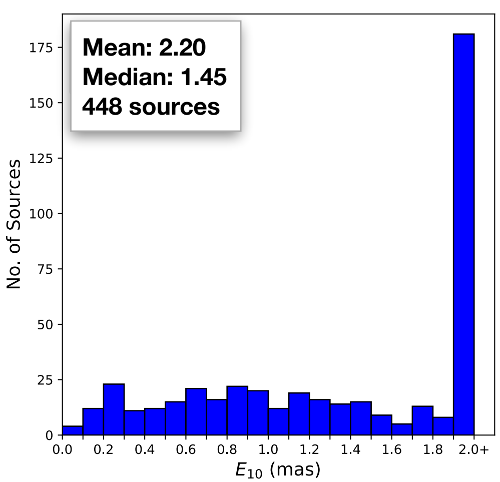

NRAO140: 3.04 mas

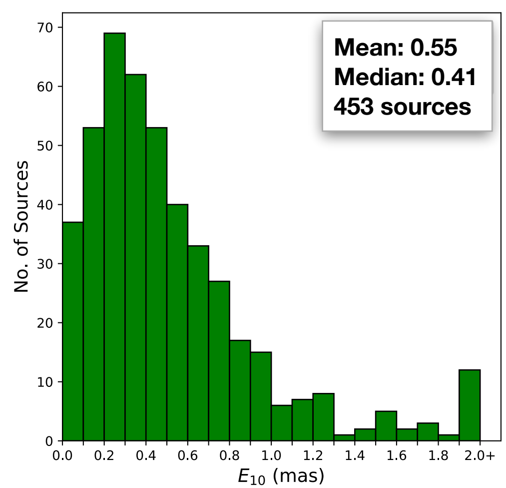

NRAO140: 1.54 mas

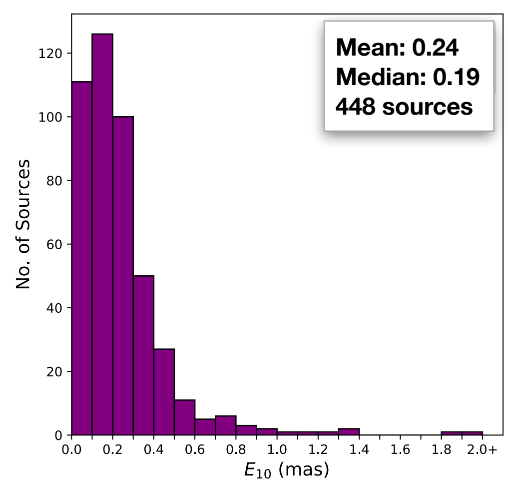

NRAO140: 0.39 mas

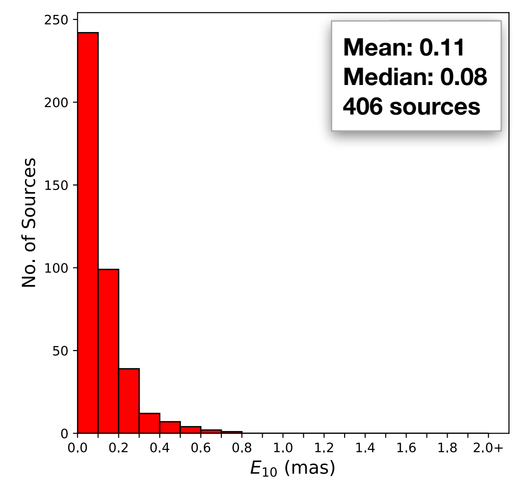

NRAO140: 0.17 mas

Structure Metrics: Radial Extent

Flux Density Weighted Radial Extent (E, mas) —> extent of structure weighted by flux

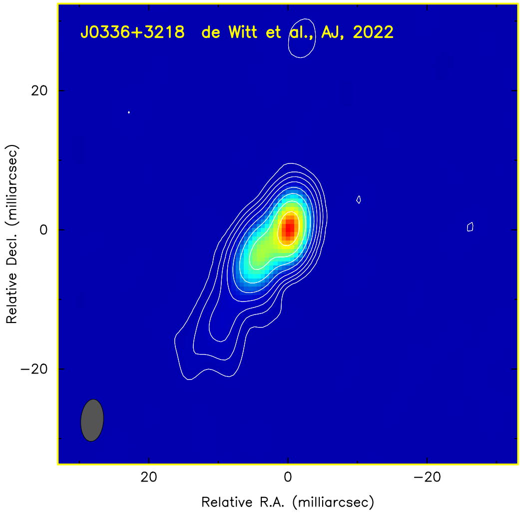

NRAO140: 4.29 mas

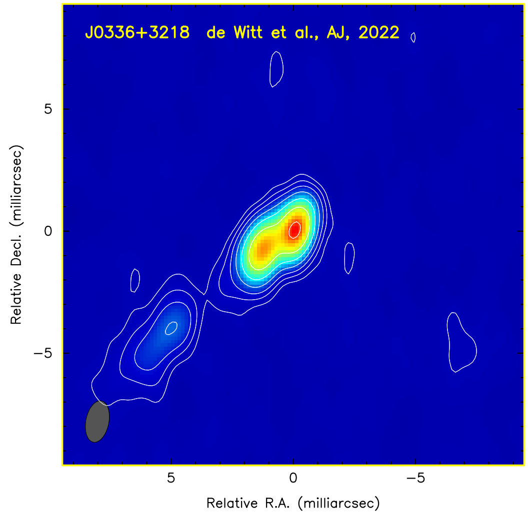

NRAO140: 1.54 mas

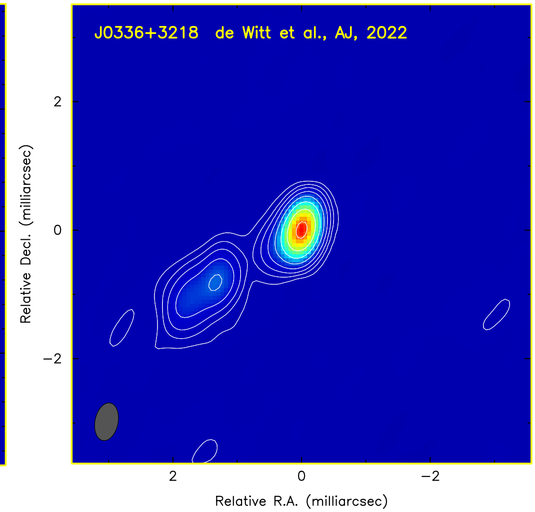

NRAO140: 0.52 mas

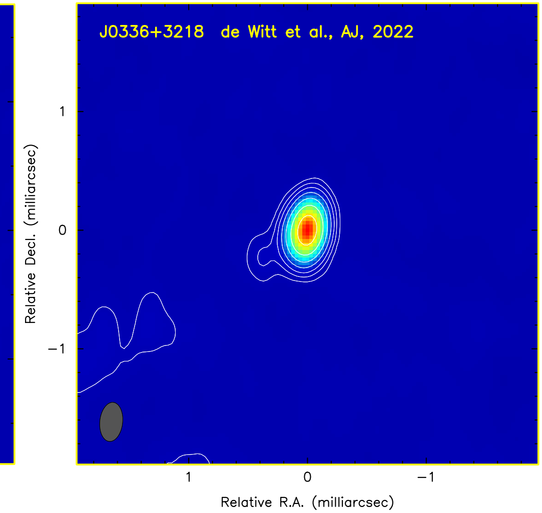

NRAO140: 0.54 mas

Flux Density Weighted Radial Extent $\leq 10 \times \theta_{FWHM}$ (E_{10} , mas) —> spurious points filtered

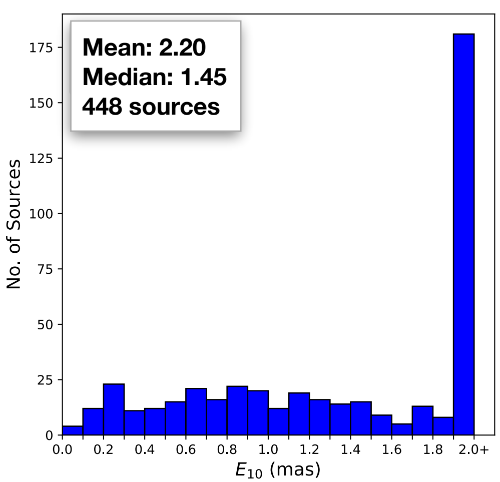

NRAO140: 3.04 mas

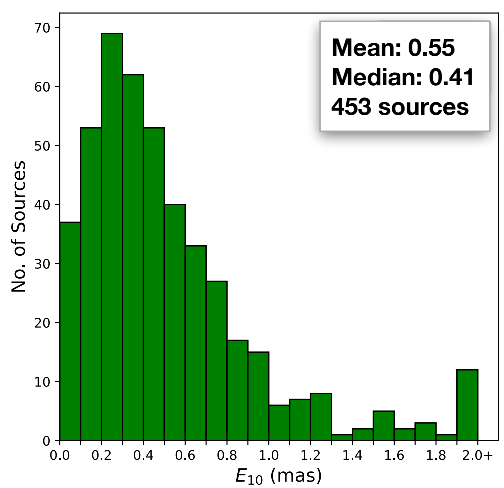

NRAO140: 1.54 mas

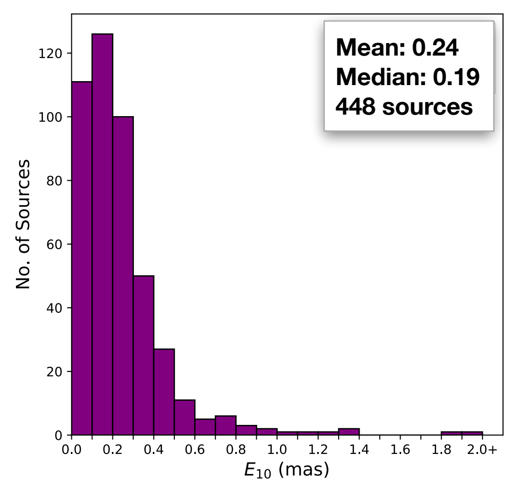

NRAO140: 0.39 mas

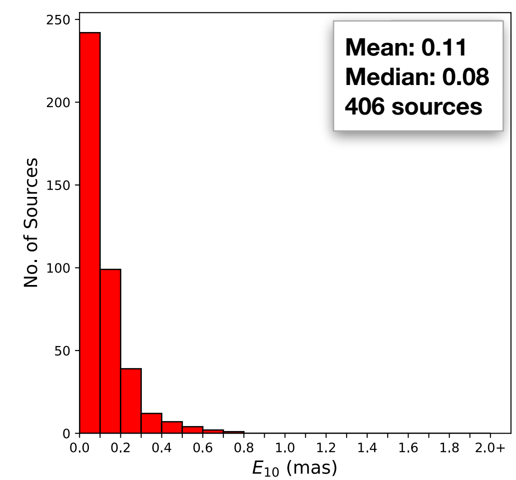

NRAO140: 0.17 mas

Astrometric Offsets: X and K-band

We compare the direction of the extended emission from modelftting to the astrometric offset direction obtained from the X and K-band α cos(δ) and δ coordinates (de Witt et al. 2022)

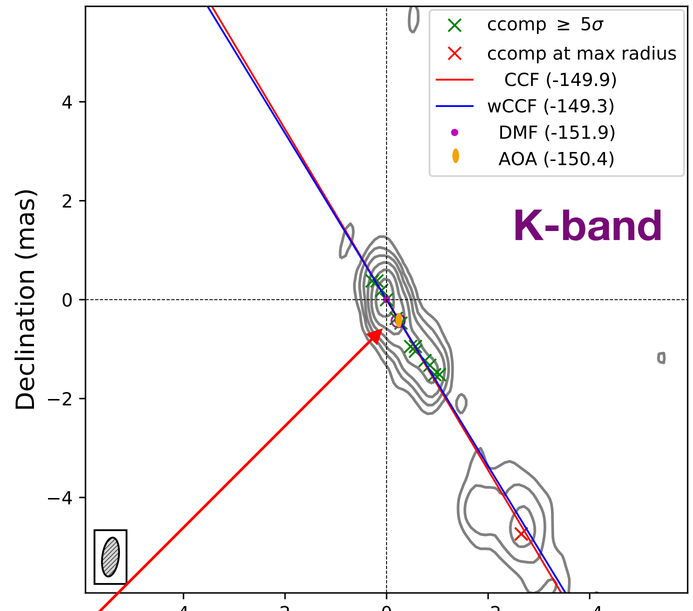

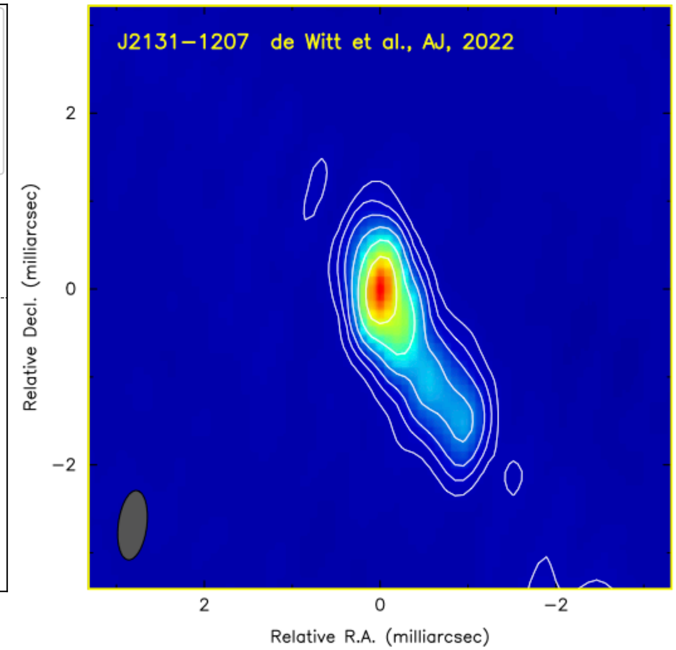

Astrometric offset at position of 2nd modelfit component

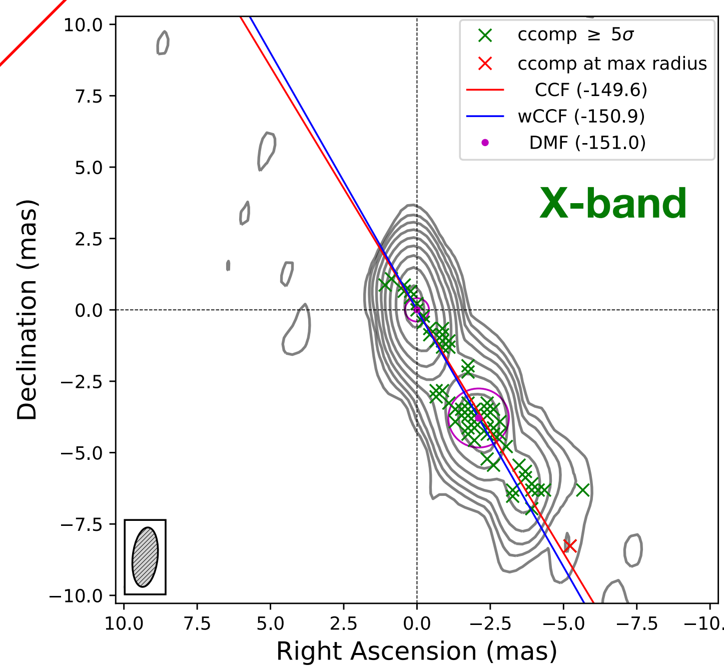

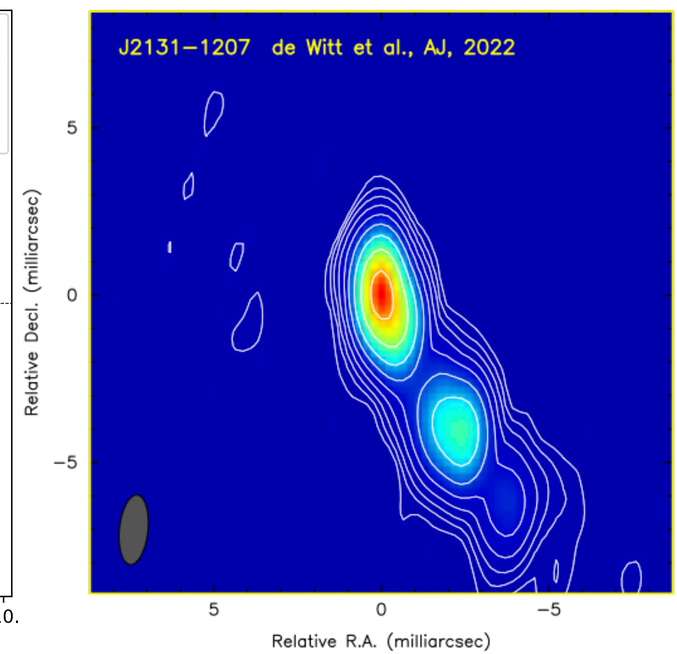

2128+123

AOA = astrometric offset angle
DMF = DIFMAP modelfit angle
CCF = angle from fit to CLEAN component locations
wCCF = angle from flux-weighted fit to CLEAN component locations.

K-band: Examples

National Research Foundation
SARAO South African Radio Astronomy Observatory

J2230+6946, strong equal double, well separated

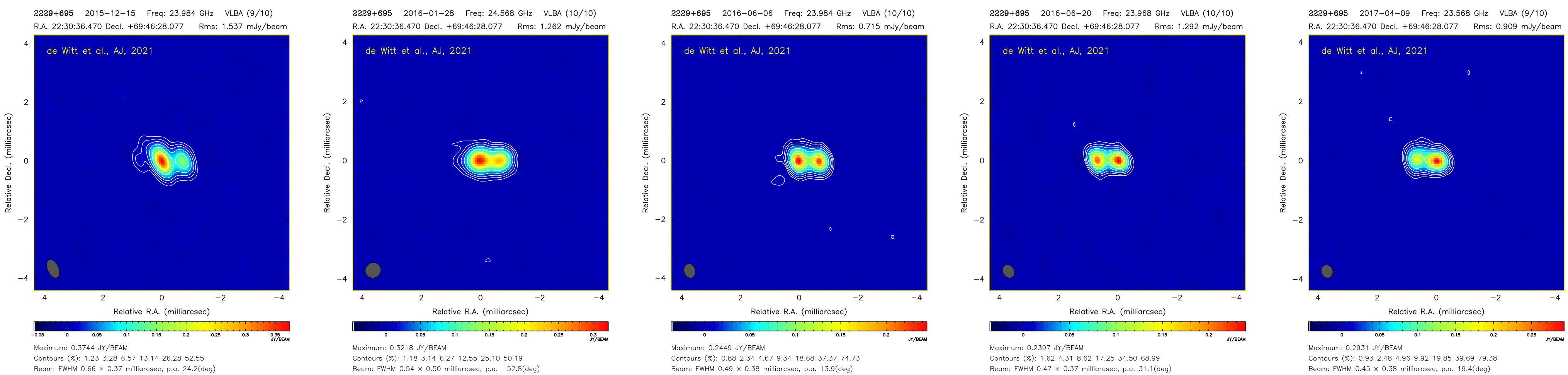

J1602+3326 and J0403+2600, triples

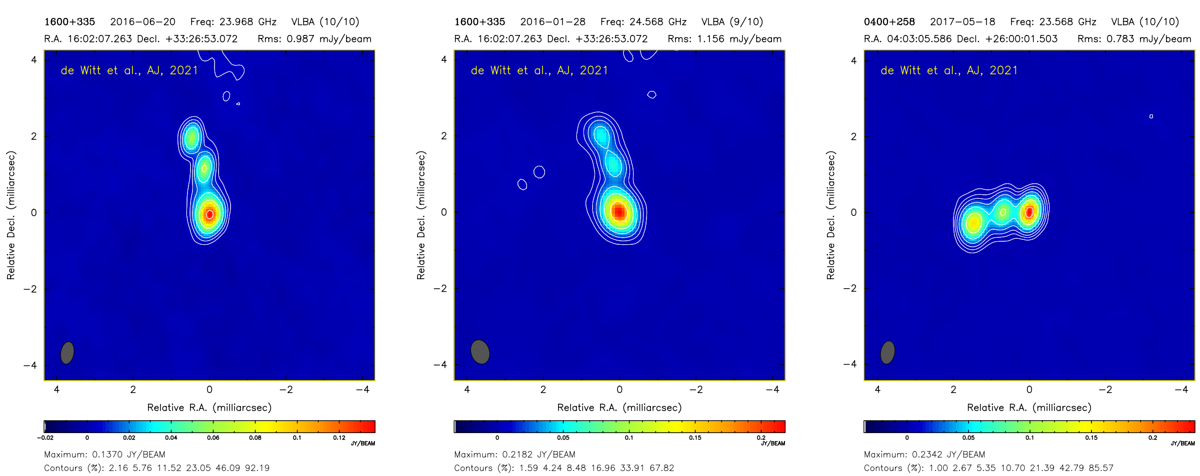

J1242+3720, strong 2nd component